1 December 1998

OPTICS COMMUNICATIONS

ELSEVIER

Optics Communications 157 (1998) 327–334

Full length article

# Diode pumped $Cr^{3+}$:LiCAF fs-laser

K.M. Gäbel [a,*], P. Rußbüldt [a], R. Lebert [a], A. Valster [b]

[a] Lehrstuhl für Lasertechnik, RWTH Aachen, Steinbachstr. 15, 52074 Aachen, Germany
[b] Philips Optoelectronics, Prof. Holstlaan 4, 5656 AA Eindhoven, The Netherlands

Received 30 April 1998; revised 17 July 1998; accepted 29 September 1998

**Abstract**

We demonstrate the first diode pumped, mode locked $Cr^{3+}$:LiCAF-laser. Transform limited 52 fs pulses were generated at 793 nm with 75 mW mode locked output power. Low loss chirped mirrors were used for dispersion compensation. Pulsed operation was achieved by Kerr lens mode locking without the need for additional cavity elements. Sub-30 fs pulses could be produced with low transmission output couplers. The laser delivered 165 mW CW-power when pumped by two laser diodes with a total of 630 mW. 

*Keywords:* fs-Lasers; Diode-pumping; Kerr lens mode locking; Chirped mirrors; $Cr^{3+}$:LiCAF

## 1. Introduction

Most of the effort, currently devoted to the development of compact fs-lasers, is focused on the diode pumpable materials $Cr^{3+}$:LiSAF and $Cr^{3+}$:LiSGaF. Pumping with high-brightness laser diodes emitting from a $\leq 100$ μm stripe has led to sub-100 fs pulses generated with each of the materials at an output power up to 125 mW [1–3]. The highest mode locked output power of 500 mW was reported from a LiSAF fs-laser, pumped by a diode-laser array [4]. The smallest wavelength at which fs-operation has been achieved is 810 nm [1]. It is believed that this limit is imposed by excessive ground state absorption. Extending the operating wavelength of diode pumped fs-lasers to smaller wavelengths in the vicinity of the Ti:sapphire gain peak is challenging since: (a) the replacement of the Ti:sapphire oscillator in CPA systems by a compact, diode pumped source is attractive because ultrafast large aperture amplifiers are mostly based on this material, large aperture $Cr^{3+}$:LiSAF amplifiers have been demonstrated at the joule level but have not found widespread use [5,6]; (b) harmonics of compact fs-sources are attractive candidates to seed ultrafast UV-eximer amplifiers [7] but none of the fundamentals in the 800–900 nm range match to multiples of eximer wavelengths; (c) 780 nm is the current operating wavelength of two-photon confocal microscopes.

We report what is to our knowledge the first diode pumped fs-laser operating at a wavelength below 800 nm. $Cr^{3+}$:LiCAF was utilized as the gain medium since its emission band is blue shifted compared to LiSAF, LiSGaF. LiCAF has been demonstrated to lase from 720–850 nm [8], it has been pumped with 670 nm laser diodes [9], and it has been mode locked delivering 170 fs pulses when pumped with a Kr-ion laser [10]. Although LiCAF was the first material of the colquiriite family the younger materials were readily adopted due to their lower optical loss and higher emission cross-section. Higher scatter loss of the laser crystal can be tolerated if the loss of the dispersive delay line, required for fs-pulse generation, can be reduced. Moreover, the lower emission cross-section of LiCAF which only affects threshold is partially compensated by the two to three times higher fluorescence lifetime. On the other hand the larger quantum-defect limited efficiency, higher thermal conductivity, lower upper state lifetime quenching, and reduced excited state absorption favor LiCAF over LiSAF, LiSGaF [11]. The weak polarization dependence of the absorption cross-section should support a small, well-matched gain volume when end

* Corresponding author. E-mail: gaebel@ilt.fhg.de

0030-4018/98/$ - see front matter 
PII: S0030-4018(98)00526-4

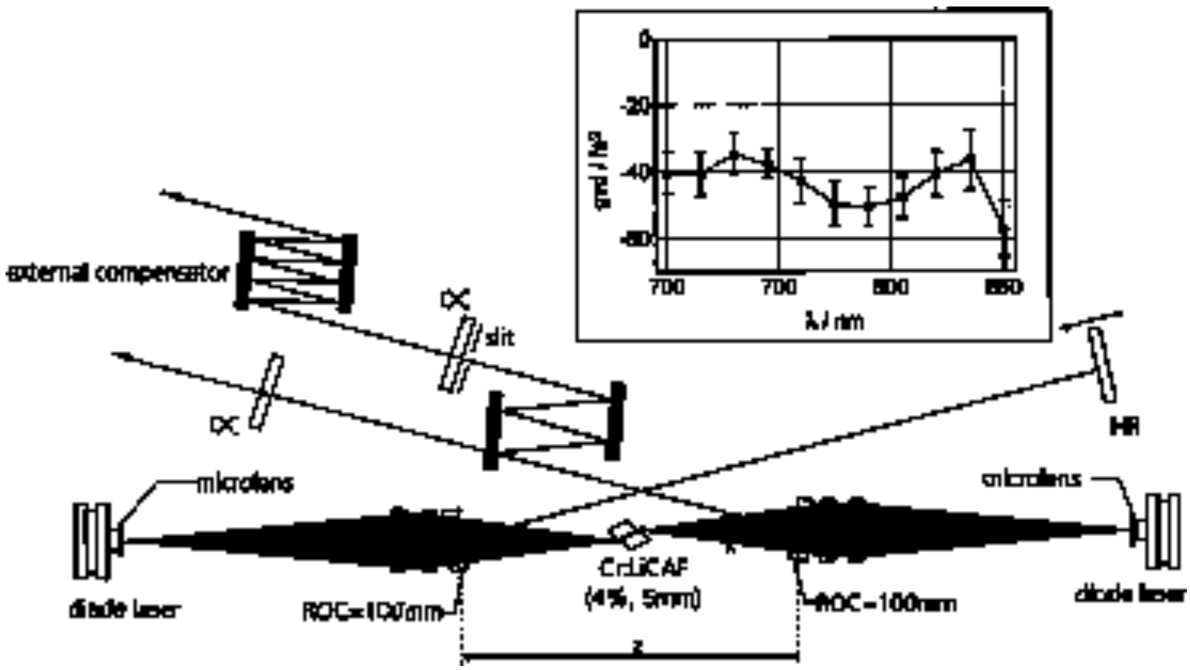


Fig. 1. Schematic of the Cr:LiCAF fs-laser; chirped mirrors are highlighted grey, grey lines represent the CW-setup, the inset shows the measured group velocity dispersion (GVD) of the chirped mirrors and associated error bars (data appear courtesy of G. Tempea, Technische Universität Wien).

pumped by polarization combined pump sources. A matched gain volume, which is equally well achieved for orthogonal pump polarization, is especially important for Kerr lens mode locked lasers which rely on an increased gain of the fs-cavity mode due to its smaller cross-section in the laser crystal.

## 2. Experimental and discussion

Our current setup, shown in Fig. 1, consists of a $x$-fold cavity which is pumped through the folding mirrors from each side by one 500 mW Philips diode laser of 50 μm stripe width emitting at 680 nm. A microlens is used to match the diode divergence in the fast and slow axis. Two achromats ($f = 120$ mm and $f = 100$ mm) are employed to collimate the beam and focus it into the laser crystal. The waist diameter of the pump beam, measured behind both achromats and the curved mirror, is 40 μm in the plane orthogonal to the diode junction and 80 μm in the parallel plane. The measured dimensions agree well with the results of ZEMAX calculations. About 320 mW pump power are available at the laser crystal from each side. The LiCAF crystal is 5 mm long with two Brewster-cut faces, has 4% nominal $Cr^{3+}$ doping and absorbs 97% of the pump radiation. Sputtered chirped mirrors were used for dispersion compensation. First we aligned the laser without the chirped mirrors to determine threshold, slope efficiency and loss in CW-operation. The threshold was determined with three different output couplers and one setup containing only HR-mirrors. The output coupler transmission was measured over the whole reflectivity band, the values given correspond to the transmission at 784 nm. From the Findlay–Clay plot shown in Fig. 2 we inferred a total cavity loss, laser crystal and mirrors, of 5.5‰. With a 1.95% output coupler we achieved a maximum output power of 165 mW when pumped with two diodes with a total absorbed pump power of 630 mW. The wavelength of

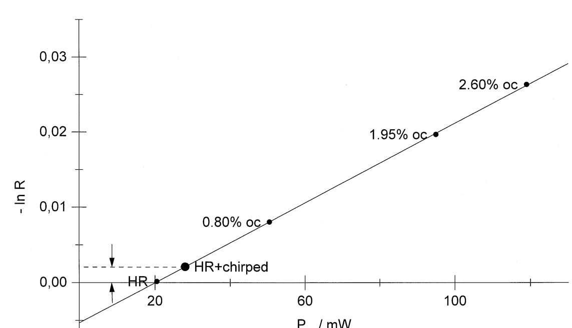


Fig. 2. Findlay–Clay plot for the Cr:LiCAF-laser, small dots represent data points measured without chirped mirrors, the large dot corresponds to eight chirped mirror reflections per round trip in a setup containing only HR-mirrors.

the CW-laser peaks at 784 nm which is consistent with the published tuning curve [8]. The laser threshold is 95 mW, the slope efficiency is 31%. Taking into account the measured cavity loss an intrinsic slope efficiency of 41% is calculated. This value indicates a slightly inferior mode matching of our diode pumped laser compared to a Kr-ion pumped system which yielded 67% intrinsic efficiency [8]. After insertion of the chirped mirrors the threshold of the setup containing only HR-mirrors was remeasured. The data point is intentionally set on the fit-line in the Findlay–Clay plot, the additional output coupling is interpreted as the loss caused by eight chirped mirror reflections. The loss per reflection is less than 0.4‰.

The chirped mirrors are identical to those which we previously utilized to compensate a LiSGaF fs-laser [12]. The GVD, shown as an inset in Fig. 1, was measured with a white light interferometer at the Technische Universität Wien. Note that a weak local minimum of $-50$ fs$^2$ is located at about 790 nm. The LiCAF-GVD was measured at the Research Institut for Solid State Physics Budapest, for details on the measurement see Ref. [13]. We calculated that eight chirped mirror reflections per round trip result in a cavity net GVD $(D)$ of $\sim -100$ fs$^2$ at 790 nm.

Optimization of the KLM cavity was performed using the matrix formalism by Magni et al. [14]. Collimated cavity arms of identical length were chosen to maximize the self amplitude modulation (SAM). The calculated values of the curved mirror separation $(z \sim 106.2$ mm), and the distance of the crystal surface from the curved mirror of the arm containing the aperture $(x \sim 52$ mm) were fine tuned experimentally to optimize Kerr lens mode locking.

An external chirped mirror pair is used to compensate the output coupler substrate and the substrates in the autocorrelator. Additional glass was placed in one autocorrelator arm to equalize the GVD of both arms which was initially different due to the beam splitter.

Using a 1.95% output coupler, transform limited 52 fs pulses were generated with an average mode locked power of 75 mW at 95 MHz repetition rate. Mode locking is initiated by longitudinally translating the HR mirror which was mounted on a stage. Once initiated the mode locking is stable over hours and stops only due to environmental perturbations. The threshold intracavity power for mode locking is $\sim 2.5$ W depending somewhat on the distance from the stability boundary. The mode locked spectrum, centered at 793 nm, is given in Fig. 3 together with the interferometric autocorrelation. The pulse width is derived assuming a sech$^2$ pulse intensity shape. The mode locked peak is about 10 nm redshifted against the wavelength of the CW-laser and coincides with the position of the largest negative cavity net dispersion $D$. This is similar to the tuning behavior of Gires–Tournois mirror controlled fs-lasers [15]. The spectrum could be slightly tuned by translating the slit in front of the output coupler. This tuning is very likely due to a weak spatial chirp caused by either dispersion in the laser crystal or the non-normal incidence

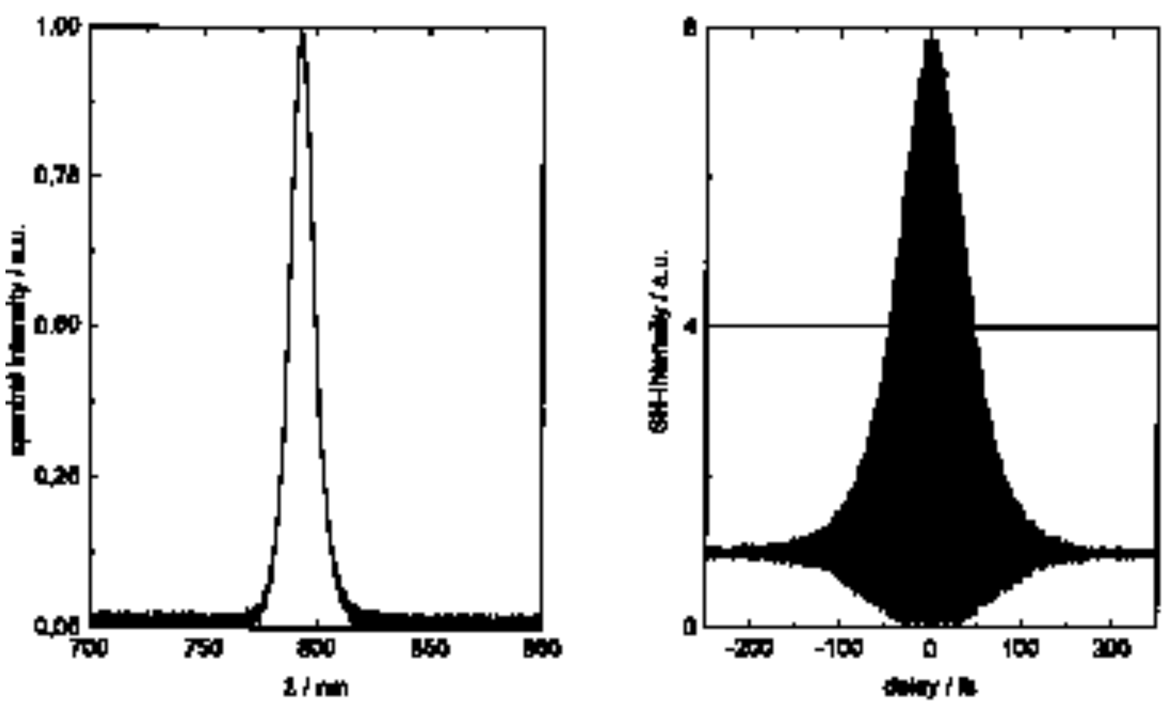


Fig. 3. Spectrum (a) and interferometric autocorrelation (b) recorded with a 1.95% output coupler and eight chirped mirror reflections; $\tau_{pulse} = 52$ fs, $\tau \Delta \nu = 0.315$.

Table 1
Summary of experimental results obtained with different output couplers and different numbers of chirped mirror reflections per round trip

| Number of chirped mirror reflections | Output coupler transmission (%) | Pulse width (fs) (deconvolution factor) | Intracavity pulse energy (nJ) | Central wavelength (nm) | $\tau\Delta\nu$ |
|---|---|---|---|---|---|
| 7 | 0.8 | 40 | 60 | 793 | 0.33 |
| 8 | 1.95 | 52 | 40 | 787–793 | 0.32 |
| | 0.8 | 29 (1.82) | 56 | 810 | 0.48 |
| | 0.1 | 20 (1.56) | 137 | 820 | 0.66 |
| 9 | 1.95 | 75 | 40 | 793 | 0.32 |

at the chirped mirrors [16]. The smallest wavelength at which sub-100 fs pulses were generated is 787 nm.

With nine intracavity chirped mirror reflections and an otherwise identical cavity we obtained 75 fs pulses with the same output power (see Table 1).

A reduction of the number of chirped mirror reflections to seven resulted in 50 mW of 40 fs pulses obtained with a 0.8% output coupler. The most striking features are two almost symmetric side bands which are 80 nm separated from each other. These side bands are caused by a dispersive wave phase matched by fourth order dispersion (FOD) of the chirped mirrors [17,18]. A slight asymmetry is due to a weak third order dispersion (TOD) contribution.

Pulses of 29 fs duration were obtained with eight chirped mirror reflections per round trip and a 0.8% output coupler. The output power was 43 mW, the time–band width product 0.48. The mode locked spectrum is red-shifted and peaks at 810 nm. Fig. 4a shows the measured spectrum, Fig. 4b gives the measured interferometric autocorrelation which has a FWHM of 52.5 fs. Since the shape of the spectrum deviates from $sech^2$, we Fourier-transformed it to calculate the pulse and the autocorrelation. For the calculation we assumed *transform limited pulses* [1]. From the calculated pulse and autocorrelation a deconvolution factor of 1.82 is derived, which is slightly smaller than for $sech^2$-pulses [2].

The shortest pulses were generated with eight chirped mirror reflections and a 0.1% output coupler. The mode locked power was 13 mW. Shown in Fig. 5a is the spectrum, Fig. 5b shows the measured interferometric autocorrelation which has a FWHM of 31.5 fs. The spectrum was assumed to be transform limited ($\Phi(\omega) = \text{const}$). The pulse, characterized by $I(t)$ and $\Phi(t)$, is derived from the Fourier-transform of the experimental spectrum and the interferometric autocorrelation is calculated. Fig. 6 gives the input spectrum for the calculation, the calculated pulse in the time domain and the envelope of the calculated interferometric autocorrelation in comparison with the experimental result. The calculated envelope fits very well to the measured autocorrelation if a FWHM of 20 fs of $I(t)$ is used. Note that the central peak is almost chirp-free and that the nonlinear chirp is accumulated in the pre- and post-cursors which contain together about 10% of the total energy. A pronounced dip is found at the center of gravity of the spectrum, which manifests itself as a modulation of the pulse in the time domain. Similar spectra were observed by other groups [19,20] and explained with a positive $D$ at the position of the dip [21]. In our laser the position of the dip coincides with the point of the lowest $|D|$, where $D$ is still negative ($\sim -25$ fs$^2$). Our interpretation is that the dip appears once the value of $D$ drops below the limit set by solitary stability, which is found at larger $|D|$ in colquiriite KLM-lasers due to the weaker SAM [12]. The observed side band is attributed to a dispersive wave which is phase matched with the blue lobe of the mode locked spectrum.

Since the spatial chirp is very low in a mirror dispersion controlled laser, the measurement of the cavity net dispersion according to Ref. [22] is not applicable. We calculated the cavity net dispersion from the position of the experimentally observed side bands [16]. The measured chirped mirror GVD was fit with a seventh degree polynomial. All cavity mirrors and 3 m air were included in the phase matching calculations. The confidence band for these calculations is determined by the HR-band edge of the curved mirrors at 735 nm and that of the chirped mirrors at 850 nm, respectively.

These calculations are illustrated in Fig. 7a and 7b for the case of seven chirped mirror reflections. Shown in Fig. 7a is the recorded spectrum, Fig. 7b gives the phase shift (GVD, TOD, FOD) versus wavelength for a spectrum centered at 795 nm. Similar calculations were performed for eight chirped mirror reflections and agreed equally well with the experimental spectra. The calculated cavity net GVD for seven and eight chirped mirror reflections is presented in Fig. 7c. Since a change in the number of the

[1] Pulses are called transform limited if the spectral phase $\Phi(\omega)$ is constant. An asymmetric spectral amplitude thus results in chirped pulses in the time domain. For a more detailed discussion see Ref. [24].

[2] Note that the deconvolution factor is interpreted as the ratio of the FWHMs of the interferometric autocorrelation and the pulse intensity. The deconvolution factor of $sech^2$ pulses (intensity) is 1.88, contrary to the usually given ratio of the FWHMs of the background free autocorrelation and the pulse intensity which is 1.54.

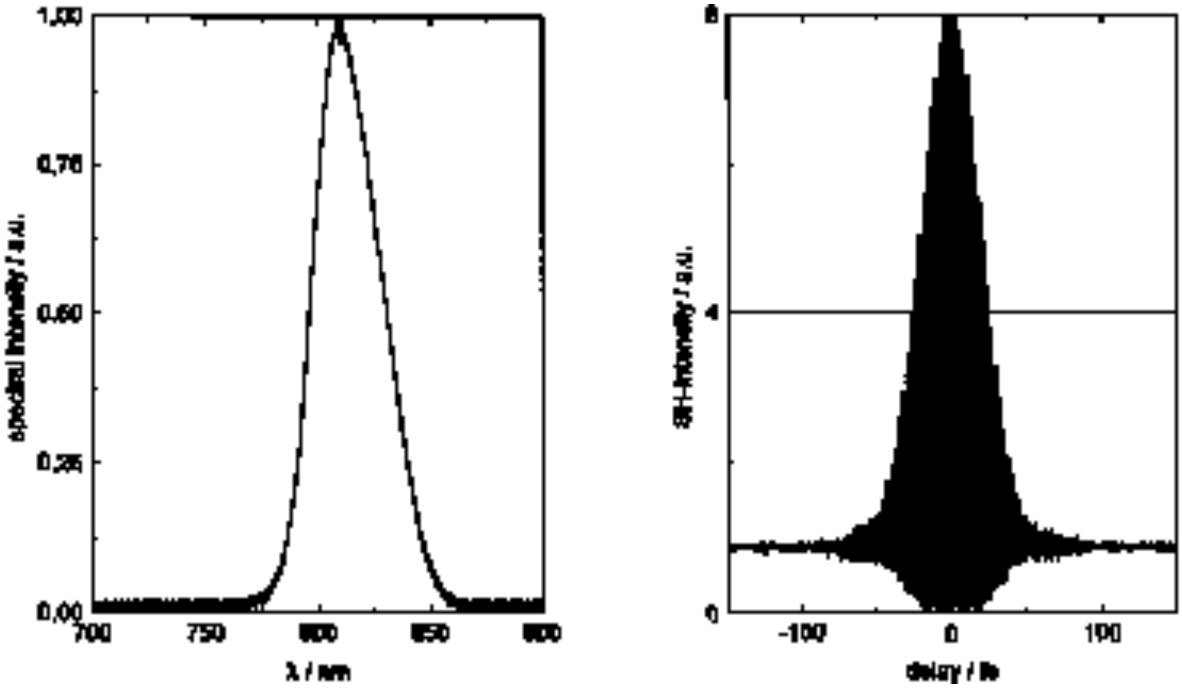


Fig. 4. Spectrum (a) and interferometric autocorrelation (b) recorded with a 0.8% output coupler and eight chirped mirror reflections, $\tau_{pulse} = 29$ fs, $\tau \cdot \Delta\nu = 0.48$.

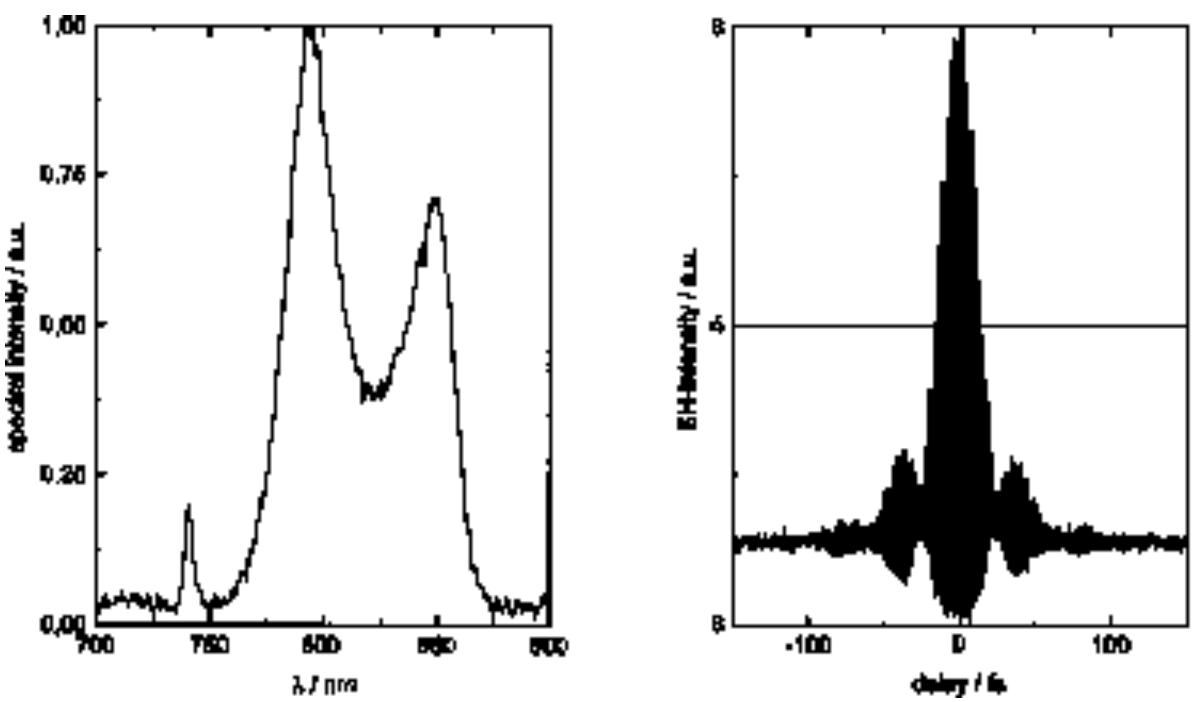


Fig. 5. Spectrum (a) and interferometric autocorrelation (b) recorded with a 0.1% output coupler and eight chirped mirror reflections, $\tau_{pulse} = 20$ fs, $\tau\Delta\nu = 0.66$.

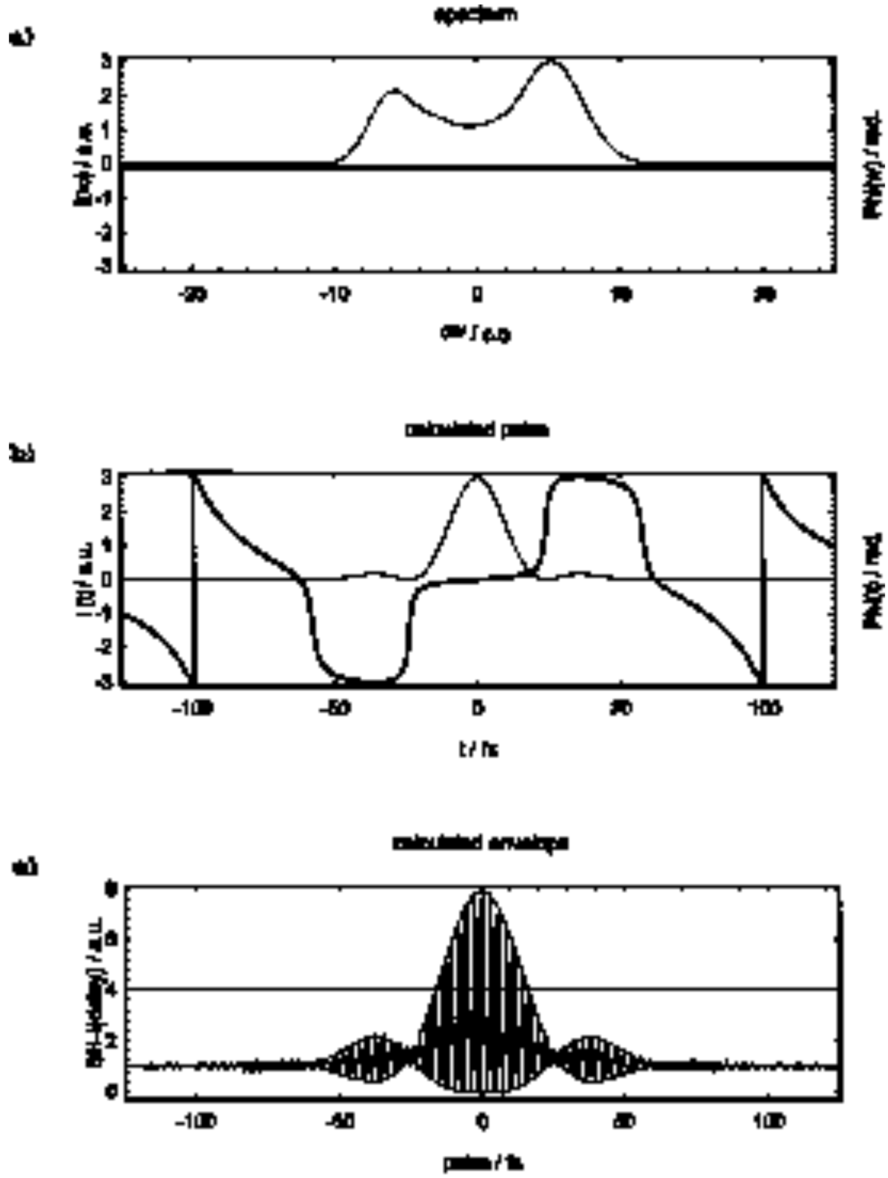


Fig. 6. Comparison of the measured autocorrelation with the calculated autocorrelation envelope of a transform limited ($\Phi(\omega) = \text{const}$) 20 fs pulse having the experimental spectral intensity: (a) recorded spectral intensity $I(\omega)$ – thin with constant phase $\Phi(\omega)$ – bold; (b) Fourier-transformed spectrum in the time domain, $I(t)$ – thin, $\Phi(t)$ – bold; (c) calculated envelope and measured interferometric autocorrelation.

chirped mirror reflections is accompanied by a variation of the (net-HOD)/(net-GVD) ratio, the cavity dispersion should be reasonably accurate despite the error bars of the chirped mirror GVD measurement.

Consistent with the finding of other groups [2,20] we observe a redshift of the mode locked spectrum which scales with intracavity pulse energy. In our experiments mode locked spectra of 56 nJ pulses (0.8% output coupler) showed $\sim 25$ nm redshift, the center of gravity of the spectrum of 137 nJ pulses (0.1% output coupler) was $\sim 35$ nm redshifted. A Raman self-frequency shift was recently presented as a possible explanation for the redshift found experimentally with the shortest pulses from colquiriite lasers [23].

In our setup with the 1.95% output coupler this origin is unlikely since the 40-nJ intracavity pulse energy and the 12.6-nm width of our spectrum seem to be lower than required for the onset of the Raman shift.

In the setup with seven chirped mirror reflections the spectrum peaks at the position of the largest negative $D$

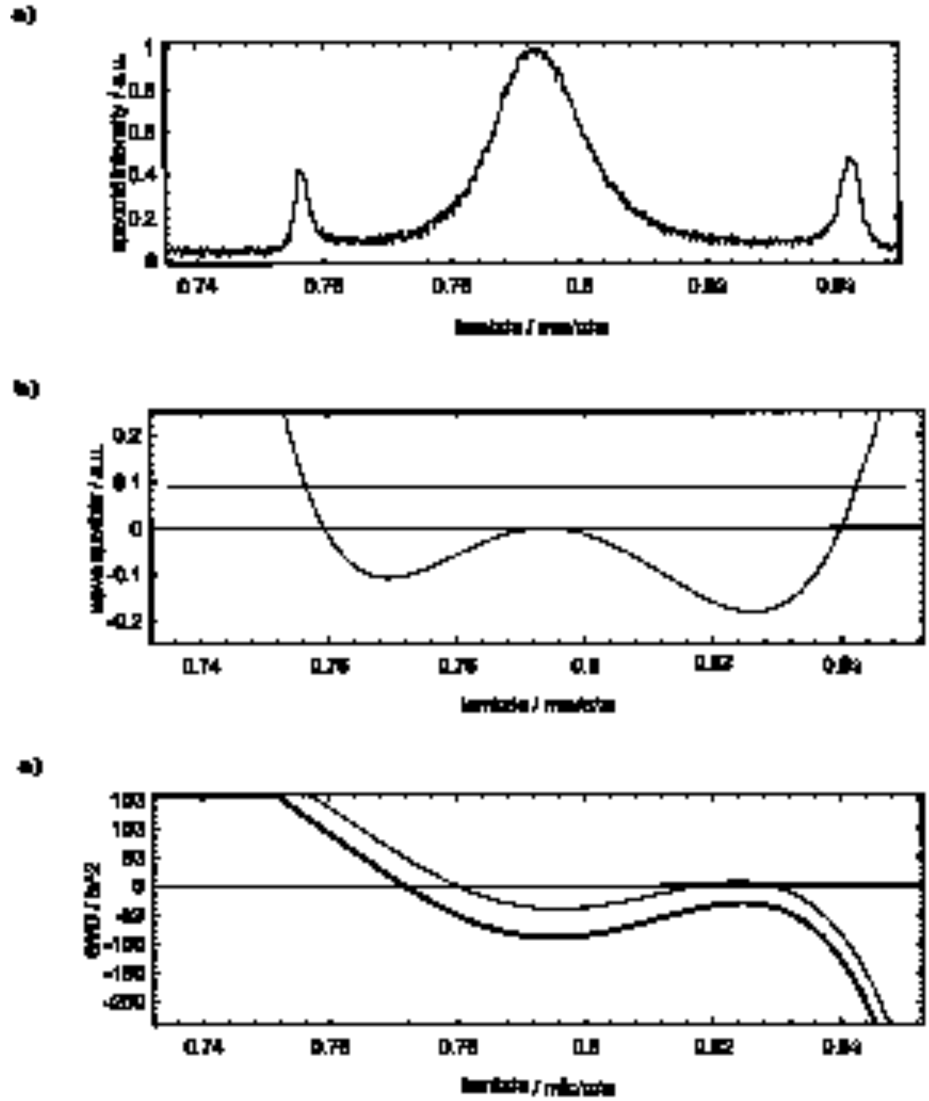


Fig. 7. (a) Spectrum recorded with seven chirped mirror reflections and a 0.8% output coupler. (b) Phase shift versus wavelength including GVD, TOD, FOD for a spectrum centered at 795 nm and seven chirped mirror reflections, the horizontal line represents a solitary wave number of 37.5 fs, side bands are located at the intersection of the solitary wave and the phase shift function. (c) Cavity net GVD with seven chirped mirror reflections – thin curve; with eight chirped mirror reflections – bold curve.

despite the relatively high pulse energy of 60 nJ. It can be explained with the small value of $D$ ($\sim -40$ fs$^2$), which is close to the solitary stability limit such that the redshift is effectively prevented by the low value of the cavity net dispersion (for the slope of $D$ see Fig. 7c).

## 3. Conclusion

In conclusion we have demonstrated the first diode pumped LiCAF fs-laser. Dispersion compensation was achieved with low loss chirped mirrors. The laser could be mode locked at a wavelength as low as 787 nm which extends the useful wavelength region of diode pumped colquiriite fs-lasers by almost 25 nm to the short wavelength side. The mode locked output power was comparable to LiSAF, LiSGaF fs-lasers, 75 mW were achieved with two pump diodes only.

The limits of the pulse width were attributed to higher order dispersion (HOD) of the chirped mirrors.

The scaling of the output power by pumping with two polarization combined diodes from each side is especially promising with LiCAF due to the weak polarization dependence of the absorption cross-section and the superior thermal and thermo-optical properties compared to other colquiriite crystals.

## Acknowledgements

The authors like to thank P. Loosen and the laser group of the Fraunhofer Institut für Lasertechnik for their kind support. We gratefully acknowledge the GVD measurement of LiCAF by R. Szipöcs and the numerous transmission measurements of cavity mirrors by H. Bette. KMG thanks M. Lenzner and K. Hehl for useful discussions. This work was performed under grant 13N7210/0 of the Bundesministerium für Bildung, Wissenschaft, Forschung und Technologie.

## References

[1] V.P. Yanowsky, F.W. Wise, A. Cassanho, H.P. Jenssen, Opt. Lett. 20 (1995) 1304.
[2] M.J.P. Dymott, A.I. Ferguson, Appl. Phys. B 65 (1997) 227.
[3] R. Mellish, S.C.W. Hyde, N.P. Barry, R. Jones, P.M.W. French, J.R. Taylor, C.J. van der Poel, A. Valster, Appl. Phys. B 65 (1997) 221.
[4] D. Kopf, K.J. Weingarten, G. Zhang, M. Moser, M.A. Emanuel, R.J. Beach, J.A. Skidmore, U. Keller, Appl. Phys. B 65 (1997) 235.
[5] P. Beaud, M.C. Richardson, E.J. Miesak, IEEE J. Quant. Electron. 31 (1995) 317.
[6] T. Ditmire, M.D. Perry, CLEO-Digest 1995, 389.
[7] Y. Nabekawa, K. Sajiki, D. Yoshitomi, K. Kondo, S. Watanabe, Opt. Lett. (1996) 647.
[8] S.A. Payne, L.L. Chase, H.W. Newkirk, L.K. Smith, W.F. Krupke, IEEE J. Quant. Electron. 24 (1988) 2243.
[9] R. Scheps, IEEE J. Quant. Electron. 27 (1991) 1968.
[10] P. Likamwa, B.H.T. Chai, A. Miller, Opt. Lett. 17 (1992) 1438.
[11] M. Stalder, M. Bass, B.H.T. Chai, J. Opt. Soc. Am. B 9 (1992) 2271.
[12] K. Gäbel, P. Rußbüldt, R. Lebert, P. Loosen, R. Poprawe, H. Heyer, A. Valster, Diode pumped, chirped mirror dispersion compensated, fs-laser, Opt. Commun. 153 (1998) 275.
[13] R. Szipöcs, A.P. Kovacs, Z. Bor, Dispersion measurement on crystals for ultrashort pulse generation with the use of interference in the frequency domain CLEO 1997, CTuP32, 1997.
[14] V. Magni, G. Cerullo, S. De Silvestri, Opt. Commun. 101 (1993) 365.
[15] I. Sorokina, E. Sorokin, E. Wintner, A. Cassanho, H.P. Jenssen, R. Szipöcs, Opt. Lett. 21 (1996) 1165.
[16] Ch. Spielmann, P. Curley, Th. Brabec, F. Krausz, IEEE J. Quant. Electron. 30 (1994) 1100.
[17] V.P. Kalosha, M. Müller, J. Herrmann, S. Gatz, J. Opt. Soc. Am. B 15 (1998) 535.
[18] I. Sorokina, Q. Lin, E. Sorokin, E. Wintner, Proceedings Advanced Solid State Lasers 19 (1998) 363.
[19] J. Zhou, G. Taft, C. Huang, M.M. Murnane, H.C. Kapteyn, I.P. Christov, Opt. Lett. 19 (1994) 1149.
[20] I. Sorokina, E. Sorokin, E. Wintner, A. Cassanho, H.P. Jenssen, R. Szipöcs, Appl. Phys. B 65 (1997) 245.
[21] I.P. Christov, M.M. Murnane, H.C. Kapteyn, J. Zhou, C. Huang, Opt. Lett. 19 (1994) 1465.
[22] W.H. Knox, Opt. Lett. 17 (1992) 514.
[23] H.A. Haus, I. Sorokina, E. Sorokin, J. Opt. Soc. Am. B 15 (1998) 1.
[24] A. Baltuska et al., Appl. Phys. B 65 (1997) 175.